View metadata, citation and similar papers at core.ac.uk
brought to you by CORE
provided by Elsevier - Publisher Connector

Developmental Cell
Resource

Systematic Screening of a *Drosophila* ORF Library In Vivo Uncovers Wnt/Wg Pathway Components

Claus Schertel,[1,7] Dashun Huang,[2,5,7] Mikael Björklund,[3,4] Johannes Bischof,[1] Dingzi Yin,[5] Rongxia Li,[5] Yi Wu,[5] Rong Zeng,[5] Jiarui Wu,[2,5] Jussi Taipale,[4,6] Haiyun Song,[5,*] and Konrad Basler[1,*]
[1]Institute of Molecular Life Sciences, University of Zurich, Zurich 8057, Switzerland
[2]School of Life Sciences, University of Science and Technology of China, Hefei 230031, China
[3]College of Life Sciences, Division of Cell and Developmental Biology, University of Dundee, Dundee DD1 5EH, Scotland, UK
[4]Genome-Scale Biology Research Program, University of Helsinki, and Department of Molecular Medicine, National Public Health Institute, Helsinki 00014, Finland
[5]Laboratory of Systems Biology, Institute for Nutritional Sciences, Shanghai Institutes for Biological Sciences, CAS, Shanghai 200031, China
[6]Department of Biosciences and Nutrition, Karolinska Institute, Stockholm 17177, Sweden
[7]These authors contributed equally to this work
*Correspondence: hysong@sibs.ac.cn (H.S.), konrad.basler@imls.uzh.ch (K.B.)
http://dx.doi.org/10.1016/j.devcel.2013.02.019

SUMMARY

We created a site-directed *UAS-ORF* library of 655 growth-regulating genes in *Drosophila*. This library represents a large collection of genes regulating cell cycle, cell size, and proliferation and will be a valuable resource for studying growth regulation in vivo. By using misexpression of genes, we prevent problems arising from genetic redundancy and can uncover novel gene functions. To validate the usefulness of this library, we screened for Wingless (Wg) pathway components. We used a combination of experimental and bioinformatic approaches to predict candidates and identified three serine/threonine kinases as regulators of Wg signaling. We show that one of these, Nek2, optimizes pathway response by direct phosphorylation of Dishevelled. In addition, we describe functional relations for roughly 5% of all *Drosophila* genes and identify a large number of genes that regulate cell size, proliferation, and final organ size upon misexpression.

INTRODUCTION

Genetic analysis relies on two complementary approaches: loss-of-function (LOF) and gain-of-function (GOF) studies. In LOF studies, the role of a gene is inferred from the phenotype that results from the partial or complete absence of its product. This is classically done by mutagenesis (St Johnston, 2002) or, more recently, by gene knockdown using RNA interference (RNAi) in vivo (Dietzl et al., 2007). However, LOF analysis alone is often not sufficient to annotate gene function due to a lack of phenotype (Rørth et al., 1998). GOF studies utilize the controlled misexpression of a gene to elucidate its function. A key advantage of this approach is the potential to identify redundant factors, whose functions overlap with those of other gene products. Functional redundancy is common in essential processes like cell cycle regulation (Buttitta and Edgar, 2007). Indeed, it has been estimated that up to 75% of *Drosophila* genes are phenotypically silent upon LOF because of genetic redundancy (Miklos and Rubin, 1996). Importantly, GOF analyses can also provide insight into pathology and evolution. Oncogenes are hyperactive in many mammalian tumors (Croce, 2008) and can be identified in overexpression studies. Additionally, GOF phenotypes can elucidate how novel gene functions evolved in different species (Cooke et al., 1997).

In *Drosophila*, two methods widely used to generate GOF situations are (1) mobilization and random insertion of P elements containing upstream activating sequences (UASs) to drive the expression of nearby genes (Rørth et al., 1998) and (2) P-element transgenesis with individual open reading frames (ORFs) under direct control of promoter sequences (Brand and Perrimon, 1993). However, the randomness of P-element insertions renders systematic overexpression approaches inefficient and prohibits direct comparisons of the effects caused by different transgenes. To overcome these limitations, we established a precisely defined in vivo library of full-length ORFs, which are integrated at a predetermined genomic position using a specific "attP" landing site. Consequently, we can reliably screen and compare the effects of expressing different transgenes. We note that, due to posttranscriptional modifications or differences in protein half-life, the abundance of the mature protein does still vary between different transgenic lines. However, for a large-scale screening approach, it is not possible to screen multiple different transgenic insertions per gene. Thus, although not perfect, the site-directed transgenic approach is the only feasible way.

To validate our library, we screened it for genes acting in growth-related signaling pathways, focusing on components of the Wnt/Wg pathway. This pathway regulates a variety of metazoan processes like patterning, growth, tissue homeostasis, and stem cell maintenance, and misregulation of it is implicated in a variety of diseases including cancer (Clevers, 2006). Many components of the Wnt pathway were identified in genetic screens in *Drosophila*. However, since the screens focused

mainly on LOF approaches, redundantly acting factors that could play important roles in regulating pathway activity might have been missed. The transcriptional output of the canonical pathway, mediated by a protein complex containing β-catenin/Armadillo (Arm) and the transcription factor TCF/Pangolin (Pan), is tightly regulated at a number of steps. In particular, key proteins are subject to numerous phosphorylation events that control the overall output of the pathway (Verheyen and Gottardi, 2010). The catalog of the kinases involved in these processes is likely to be far from complete.

It is becoming increasingly clear that there is significant crosstalk between distinct signaling pathways and thus a need to analyze this at a systems level. Our study provides an example of such an approach. By integrating data from different large-scale in vivo and cell culture screens, we can identify components of individual signaling pathways. The discovery of three Wg signaling regulators illustrates how data collected from unrelated screens can facilitate the prediction and identification of novel pathway components.

RESULTS

Library Construction

Our ORF library comprises 655 candidate growth regulatory and cell division genes. These were selected based on their LOF phenotypes in *Drosophila* S2 cells (Björklund et al., 2006) or belong to pathways and processes that have previously been linked to growth and cell division. We used the site-directed phiC31 integrase system to create transgenic lines for all the ORFs in our library. All transgenes were inserted into a landing site at cytological position 86F on the third chromosome (Bischof et al., 2007). We constructed the library in two versions: (1) a 3×HA sequence is directly fused to the ORF. The epitope tag facilitates the biochemical isolation and visualization of the proteins. However, since tags can potentially interfere with protein function, we also constructed (2) an untagged library where full-length ORFs with their native stop codons were used. Indeed, in the few cases where we saw functional differences between corresponding transgenes, the tag mostly seems to interfere with protein function leading to a false-negative result. A detailed analysis of the effects of tagging will be presented elsewhere (Bischof et al., 2013).

We retrieved strains for 578 (88%) untagged and 627 hemagglutinin (HA)-tagged ORFs (96%). Together, these strains cover 99% of all genes that were included in the ORF library (the complete list can be found in Table S1, sheet 1, available online). All clones were sequenced, and the tagged versions were verified for protein expression in S2 cells.

Using the Library for In Vivo Screens

We misexpressed each transgene in eye and wing primordia by using eye- (*ey-Gal4*) or wing-specific (*MS1096-Gal4*) Gal4-driver lines. Blind screening was performed for all lines. In cases where phenotypic differences were documented for untagged versus 3×HA-tagged strains, we recorded the more severe phenotype and used the respective strain for further screens in sensitized backgrounds. A total of 183 transgenes induced a discernible phenotype in the eye (27.9%), while 313 induced wing phenotypes (47.8%) (Table S1, sheet 1). According to the phenotypic strength, we assigned a score ranging from 0 (no phenotype) to 4 (lethality): 1 to 3 denote gradually increased growth distortions, with 3 indicating the almost complete absence of the organ. These initial screens were used to assess the quality of the library in three ways: (1) to test the functionality of the individual transgenes (at least half of our transgenes are functional as judged by their ability to induce phenotypic changes, and the remainder is most probably also functional yet phenotypically silent); (2) to test for penetrance and expressivity (the observed phenotypes with our *UAS-ORF* lines were 100% penetrant, and the expressivity between individuals was highly consistent); and (3) to identify potential dominant-negative effects. We knocked down the expression of 351 genes represented in our library using strains from the VDRC RNAi library (Dietzl et al., 2007). Of these, only 75 (21.4%) lines showed severe phenotypes (23 caused lethality), while knockdown of the vast majority of the 351 genes resulted only in mild effects that occurred with low penetrance or no phenotypes at all. Twenty-one of the 52 (40.4%) nonlethal genes that caused a severe growth deficit when knocked down also showed smaller wings when the corresponding transgenes were overexpressed, suggesting that these *UAS-ORF* lines exhibit dominant negative effects.

In sum, the data suggest that most of our transgenes are capable of yielding highly reproducible phenotypic readouts. Thus, our in vivo library provides a high-quality resource for studying cell cycle and growth regulating genes in *Drosophila*.

Screens in Genetically Sensitized Backgrounds Provide a Resource for Further Investigation

To test whether the observed growth phenotypes are dependent on apoptosis, we reduced cell death in the eye and the wing by coexpressing the *Drosophila inhibitor of apoptosis protein 1* (*diap*1) (*ey-Gal4;EPdiap*1 and *MS1096-Gal4;EPdiap*1). We found that 40% of all observed growth effects could be blocked in this way. Importantly, the remaining 60% of the lines produced growth effects that are most likely not apoptosis-related and might reflect interactions with growth promoting pathways. These genes are valuable candidates for further studies on growth regulation (see Table S1, sheet 2, for a complete list).

We also screened five different genetically sensitized backgrounds to test whether the growth effects that we observed in the wild-type tissues can be assigned to a specific pathway: (1) the Insulin Receptor (InR) (*GMR-Gal4>UAS-InR*), (2) Jak/Stat (*ey-Gal4;GMR-upd*), (3) Myc (*GMR-Gal4 UAS-Myc/SM5;2xUAS-Myc/TM6b*), (4) Hedgehog (Hh) (*salE-Gal4 UAS-smo*^{1}), and (5) Wg (*sev>wg*; Brunner et al., 1997) pathway. These screens provided us with a wealth of information about candidate components of the investigated pathways and will be a valuable resource for future research. All identified candidates and further details on each screen are presented in Table S1 and Figures S1–S3. A separate clustering for each individual screen (including all identified candidates together with the known pathway components) suggests functional relationships that can be further tested as exemplified below for the Wg pathway. We also implemented a STRING-based tool, which is available to the research community (http://clockurl.com/key/Schertel_et_al_2012a). This allows the reader to use the STRING database with a query of the reader's own choice. If the resulting

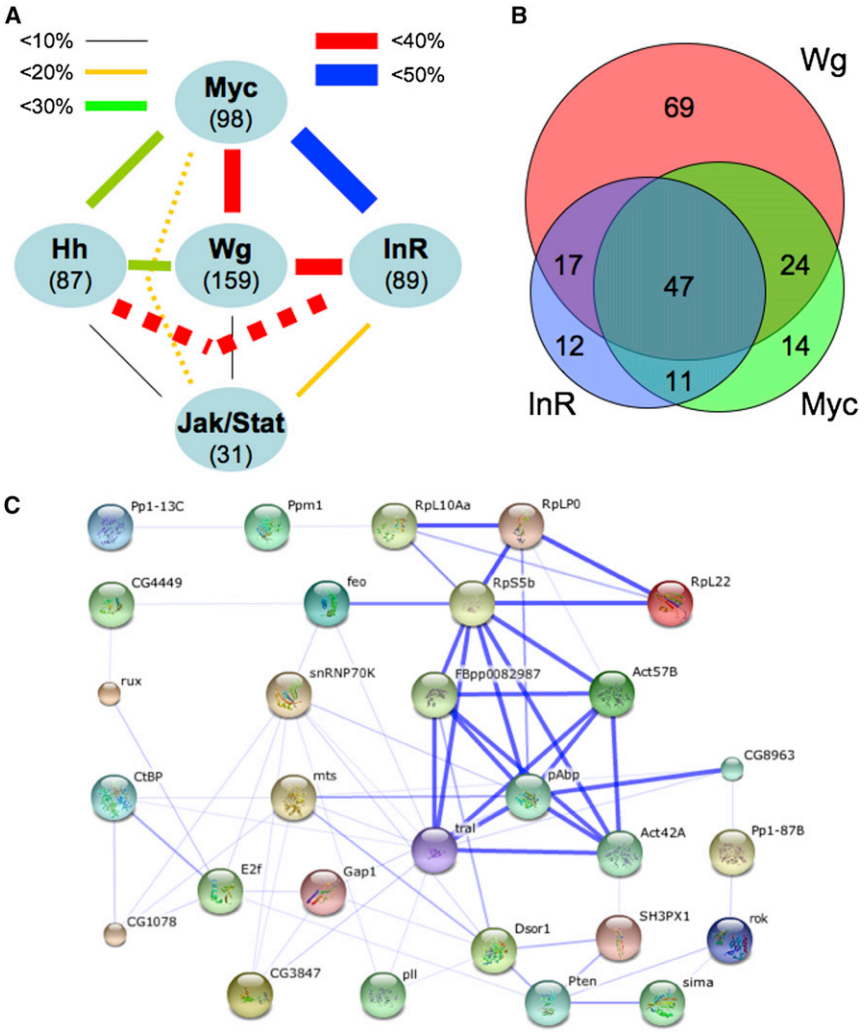

Figure 1. Analysis of Screening Data

(A) Numbers in brackets indicate the total number of positive candidates. Connecting lines are color coded according to degree of overlap. We calculated the percent overlap between the two respective candidate lists and normalized the overlap for the number of genes that are expected to overlap by chance. Since we did not test all 655 genes in all screens, we restricted the analysis to those that were tested pairwise in both assays (between 617 and 648).

(B) Venn diagram of the overlap between the three most similar screens: Myc, InR, and Wg. A total number of 635 genes was tested in all three screens.

(C) Predicted protein-protein interactions of the 47 candidates. STRING (version 9.0) predicted interactions for 29 candidates. Thickness of lines represents confidence score (minimum set to 0.15).

See also Figures S1–S3.

network contains any gene that is included in our library, STRING will highlight this gene and present the screening data connected to this gene directly to the user. Thus, any gene set of interest can be easily linked to the genes (and screening data) that were under investigation in our study. We show an example gene network built from the candidate list of a previous publication on wing development (Cruz et al., 2009).

To obtain an indication of the extent of potential crosstalk between the different pathways tested, we performed a pairwise comparison of the candidates in each screen (Figure 1A). The least overlap is found between the Hh and Jak/Stat screens and the Wg and Jak/Stat screens, suggesting that these pathways share only little mechanistic or functional relationship (Figure 1A; Table S1, sheet 2). In contrast, the most significant overlap is observed between the Myc and InR screens (59; $p < 3.5E-35$). Interestingly, there is also significant overlap of these two screens with the Wg screen. We identified 47 genes yielding phenotypes in all three screens (Figure 1B). Of these, 29 form a network on the protein level when analyzed with the STRING database, which comprises reported as well as predicted physical and functional protein interactions inferred from gene coexpression, text mining, and publicly available databases of experimental data (Jensen et al., 2009) (Figure 1C). This high interconnectivity validates the notion that the three pathways could be functionally related and that there is crosstalk between the pathways either on the level of common components or targets. Among the 47 common genes, five ($p < 0.0005$) are annotated under the Gene Ontology term "protein serine/threonine (S/T) phosphatase activity." This indicates that the three pathways are regulated by identical factors at the level of posttranslational modifications, like phosphorylation, which activate or inactivate different pathway components.

Together, the presented resources provide information for a large number of genes and possible interaction with multiple signaling pathways. It further presents testable hypotheses for functional relationships between these genes and specific signaling pathways that can be used as a starting point for further investigation to reveal additional pathway components.

Meta-Analysis of the Screening Data

As a next step, we wanted to explore the predictive power of analyzing the combination of all the screens. We reasoned that the integration of all data could result in synergistic information that exceeds the sum of the individual data. To do this, we used hierarchical clustering and predicted STRING network interactions. We illustrate how such integration of data from different approaches can be used to identify potentially novel components in a pathway of interest.

In a first step, hierarchical clustering identifies genes with similar effects in different screens. Genes that cluster in close proximity to bona fide components of the pathway of interest represent good candidates for additional pathway components. This initial candidate list is then further interrogated by

searching the STRING database for predicted protein interactions between the candidates and all known pathway components. Candidates sharing many predicted interactions with pathway components are subsequently ranked higher than genes, whose products lack such interactions. In a third step, data from a sensitized screen for the pathway of interest can be used to refine the candidate list. Here, we assign an additional score to candidates that caused a phenotypic response (suppression or enhancement) in the *sev>wg* background. We apply this adjustment after the raw data from the screens were already used in the initial clustering to prevent a strong bias in the clustering results. Each one of the three approaches alone is not specific enough to predict novel components with high confidence as evidenced by the typically large number of suppressors and enhancers identified in the in vivo screens. However, the combination of all three approaches results in a list that is enriched for high-confidence candidates. We illustrate the usefulness of this type of analysis for the Wnt/Wg signaling pathway, since there is already a large amount of data available on the components involved, as well as on their functional relationships. Moreover, our ORF library contains 24 of 49 genes (49%) that are known to encode regulators of the Wg pathway (see Table S1, sheet 3, for a complete list).

Candidate Identification by Combining Clustering and STRING Predictions

We used the data that we collected in our in vivo screens and added data from S2 cell-culture-based screens performed with the same gene set (Table S1, sheet 1, and Experimental Procedures). The Cluster algorithm (Eisen et al., 1998) groups all genes into functional classes by an unsupervised hierarchical clustering of the semiquantitative phenotypes scored in the assays. We clustered all 655 genes and all screening data and investigated the distribution of bona fide Wg pathway components within the entire clustering tree. We found a significant enrichment in three clusters. Together the three clusters contain 21 out of the 24 bona fide Wg pathway components included in our library. This enrichment suggests that other genes in these subclusters might also be involved in Wg signaling.

In particular, one cluster, which comprises only 17 genes (2.6% of all genes), is highly enriched for Wg signaling components (Figure 2C). We next ranked the genes in this cluster according to predicted interactions of their encoded proteins with Wg components. We analyzed predicted interactions of the 49 known Wg signaling pathway components with the 17 genes in the subcluster. Only two proteins showed predicted interactions with Wg signaling pathway components. The protein Nek2 is connected to multiple Wg pathway proteins. We found connections to Reptin (Rept), Arm, Dishevelled (Dsh), Axin (Axn), and Frizzled (Fz) (Figure 2D) that are based on comentioning in the literature. Interestingly, *arm* and *dsh* were also the two genes *Nek2* clustered most closely with and *fz* was in the adjacent cluster. Only one other protein, Smi35A, showed interactions with the Wg pathway components Shaggy (Sgg) and CKIα (Figure 2D). Furthermore, expression of both transgenes enhanced the *sev>wg* phenotype in the Wg-sensitized screen (Table S1, sheet 3). Combined with the clustering result and the predicted interactions this suggests an involvement of *Nek2* and *smi35A* in Wg signaling.

Overexpression of *Nek2* and *smi35A* Enhances Wg Target Gene Expression

We expressed the *Nek2* and *smi35A* transgenes in the larval wing imaginal discs and assayed the expression of Wg target genes. *en-Gal4*-driven expression of *Nek2* in the posterior compartment caused an upregulated expression of the Wg target genes *Distal-less* (*Dll*) and *senseless* (*sens*) (Figures 3C and 3D). In addition, when *Nek2* is expressed in the entire wing disc (*MS1096-Gal4*), the adult wings show a severe size reduction. Although mild Wg pathway activation leads to increased growth, it is well known that strong overactivation has the opposite effect, probably due to an increase in cell death (Baena-Lopez et al., 2009). Importantly, Nek2 causes ectopic formation of sensory bristles, a hallmark of strong ectopic Wg signaling (Figures 4B and 4E). Thus, we conclude that *Nek2* acts as a potent enhancer of Wg signaling.

Compartment-specific overexpression of *smi35A* by *en-Gal4* causes enhanced *Dll* expression compared to control compartments (Figure 3E); expression of *sens* remained unchanged (Figure 3F). Since *sens* expression requires higher Wg signaling levels than *Dll*, it seems that *smi35A* overexpression has a weaker effect on the pathway than *Nek2*. Adult wings overexpressing *smi35A* by *MS1096-Gal4* were slightly enlarged (Figure 4C), consistent with the effects of mild Wg pathway overactivation (in contrast to strong ectopic activation). Together, the data indicate that *smi35A* encodes a positive regulator of the Wg pathway.

Screening for Additional S/T Kinases Involved in Wg Signaling

Since both *Nek2* and *smi35A* possess S/T-kinase domains, we searched our library for additional S/T kinases and identified 41 genes, including four known Wg components: Sgg, Gish, CKIα, and CKIIα. Since kinases typically have multiple targets that might act in different pathways, the kinases are spread out in the clustering tree. For example, CKI and Sgg are also involved in Hh signaling (Jia et al., 2002, 2004), which might prevent close clustering exclusively with Wg components. Thus, we refined our candidate search and included the Wg screen data to get better candidate predictions. We combined the clustering, protein interaction, and Wg screen data for all S/T kinases and ranked them accordingly (see Experimental Procedures for details). The only candidate gene that scored in all three categories was the MAPK *licorne* (*lic*) (Table S2). In the clustering tree, *lic* clusters closely with *CKIα* and *gish* (Figures 2A and 2B). Furthermore, it has one predicted interaction with the phosphatase Mts (Figure 2D). We tested two candidate genes, *lic* and *Mekk1*, in the imaginal disc setup. Although it ranked lower in the candidate list, we chose to test *Mekk1* because it also encodes a MAPK and thus allows us to examine if the MAPK cascade might have a general effect on Wg signaling.

Expression of *lic* by *en-Gal4* represses both *Dll* and *sens* in the posterior compartment (Figures 3G and 3H). This argues for an additional negative role in Wg signaling besides a function in the MAPK pathway. *Mekk1* misexpression did not have a specific effect on Wg target gene expression arguing against a general effect of the MAPK pathway on Wg signaling. Overexpression of *lic* by *MS1096-Gal4* results in smaller wings that show vein-patterning defects (Figure 4D). In particular, the anterior and posterior cross-veins are mostly absent in these wings.

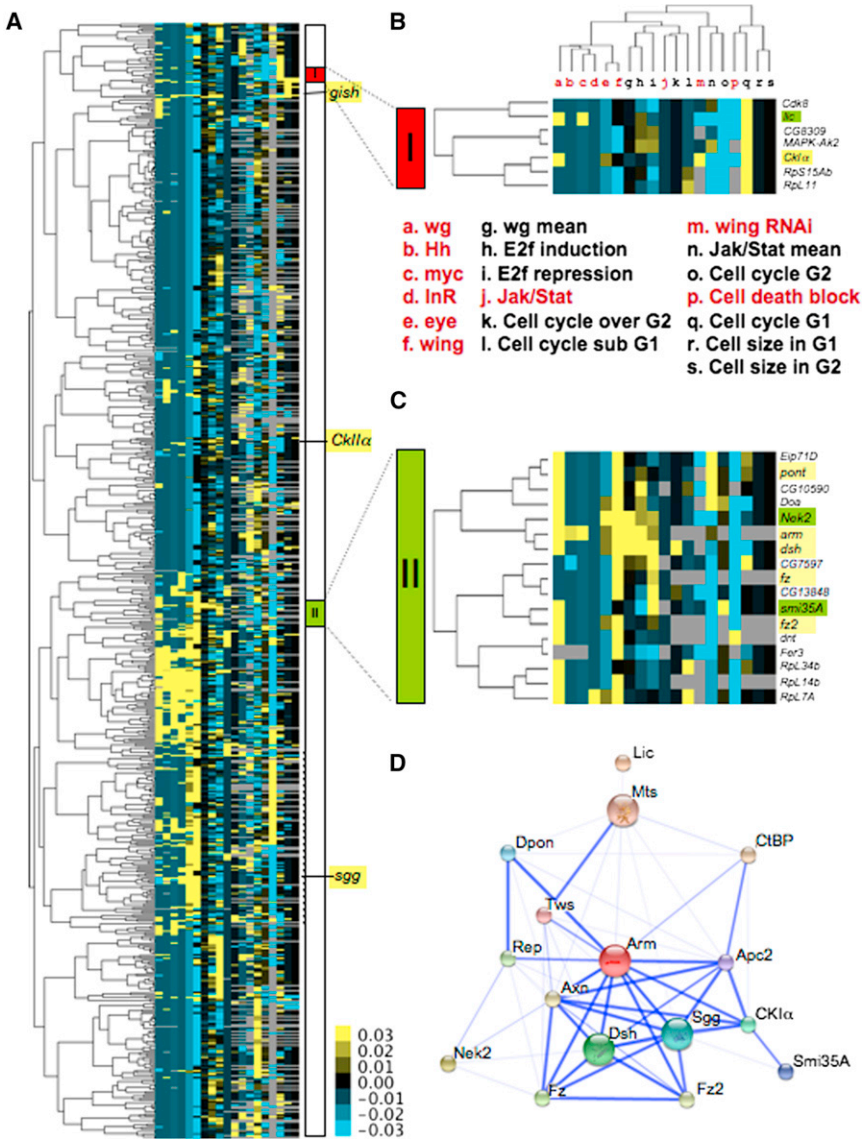

Figure 2. Clustering Results

(A) Hierarchical clustering of all genes across all assays. The location of the clusters containing *Nek2*, *smi35A*, and *lic* are indicated by colored boxes and enlarged in (B) and (C). The location of the four bona fide Wg pathway kinases is indicated on the right. The normalized scale bar for the clustering is indicated at the bottom right. We scored phenotypic strength in the in vivo assays on a scale ranging from 1 to 3 (positive and negative values for enhancers and suppressors). A lethal phenotype was scored as 4. If the phenotype was suppressed by *EPdiap1* (cell death block), we assigned a 1, otherwise, we assigned a 0.

(B and C) Enlarged views of the colored regions indicated in (A). Confirmed candidates are shaded in green, and previously known Wg components are shaded in yellow. The clustering of the different assays is displayed on top. The assays are as follows: a. *ey-flp;ey-Gal4;sev>y+>wg*. b. *salE-Gal4 UAS-smo*. c. *GMR-Gal4 UAS-Myc/SM5;2xUAS-Myc/TM6b*. d. *GMR-Gal4 UAS-InR*. e. *ey-Gal4*. f. *MS1096-Gal4*. g. Wg reporter assay by RNAi (S2R+ cells). h. E2f reporter induction (S2 cells). i. E2f reporter repressed (S2 cells). j. *ey-Gal4;GMR-upd*. k. Over G2 phenotype strength by RNAi (S2 cells). l. Sub G1 phenotype strength by RNAi (S2 cells). m. *MS1096-Gal* with RNAi. n. Jak/Stat reporter assay (S2 cells). o. Sub G2 phenotype strength by RNAi (S2 cells). p. Cell death block by *EPdiap1*. q. G1 phenotype strength by RNAi (S2 cells). r. Cell size in G1 phenotype strength by RNAi (S2 cells). s. Cell size in G2 phenotype strength by RNAi (S2 cells) (for details about the cell-based screens, see Björklund et al., 2006).

(D) STRING (version 8.3)-based network of predicted protein interactions for Nek2, Lic, and Smi35A with all interacting Wg signaling pathway components. Thickness of the edges corresponds to confidence score. The following hyperlink allows readers to browse the network in STRING: http://clockurl.com/key/Schertel_et_al_2012a. See also Figures S1–S3 and Tables S1 and S2.

Expression by *hh-Gal4* leads to an overall smaller adult wing (Figure 4G).

Specificity of the Observed Effects

To test whether the observed effects occur downstream of *wg*, we examined if overexpression of our candidates altered *wg* expression. Importantly, since *wg* itself is not a target of the Wg pathway, it also serves as a control for a general effect on transcription. When we expressed *Nek2*, *smi35A*, or *lic* using the *en-Gal4* driver, we observed no change of *wg* expression (Figures 3D′, 3F′, and 3H′). These findings indicate that all three genes have a specific function in Wg signaling rather than a general effect on transcription or a specific effect on *wg* expression. Furthermore, we did not detect an effect of *Nek2* on the expression of the Notch target *cut* arguing for a specific function in the Wg pathway (data not shown).

Since the identified genes encode kinases, we wanted to test whether the kinase activity is required for the observed phenotypes. We created transgenic lines that express a mutant version of each gene in which the kinase domain is rendered nonfunctional by mutation of a conserved lysine in the VAIK motif present in the kinase domain (Varjosalo et al., 2008). *Nek2* overexpression induced ectopic sensory bristles (Figure 4E). However, the kinase-dead $Nek2^{K48M}$ version was not able to induce such an effect (Figure 4H). Similar results were observed for wild-type *smi35A* and $smi35A^{K227M}$ and for wild-type *lic* and lic^{K75M} (Figures 4F–4J). Given that wild-type and mutant constructs are expressed at comparable levels (Figure 4K), these findings indicate that indeed the enzymatic activity of the S/T kinases is responsible for the observed effects on Wg signaling.

No Effect of *Nek2*, *smi35A*, or *lic* Knockdown on Wg Target Expression

Since our overexpression analysis indicated that all three genes can alter the Wg pathway output, we wanted to determine if they are also necessary for normal development. To this end, we

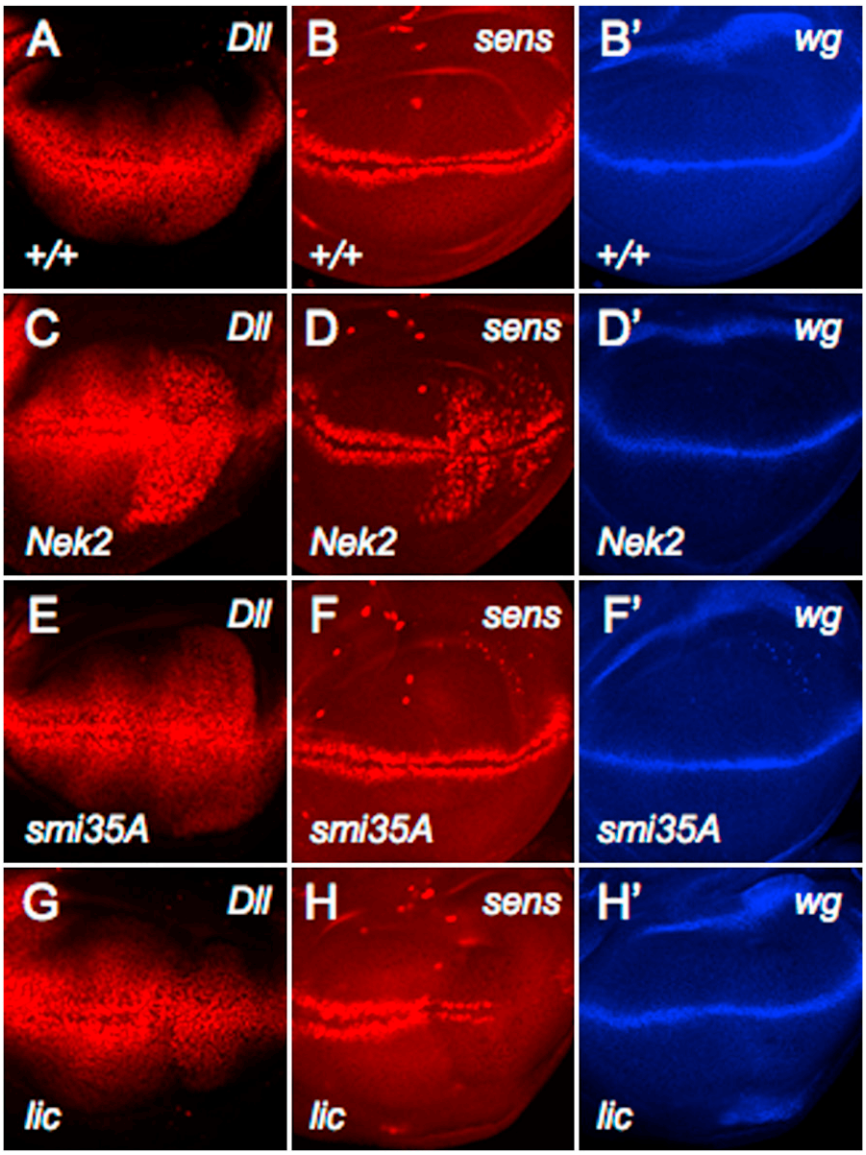

Figure 3. *Nek2*, *smi35A*, and *lic* Act Specifically on Wg Targets
(A) *en-Gal4* control: α-Dll staining.
(B) *en-Gal4* control: α-Sens.
(B') *en-Gal4* control: α-Wg; same disc as in B.
(C) *en-Gal4, tubGal80^{ts} UAS-Nek2HA*; α-Dll.
(D) *en-Gal4, tubGal80^{ts} UAS-Nek2HA*; α-Sens.
(D') *en-Gal4, tubGal80^{ts} UAS-Nek2HA*; α-Wg.
(E) *en-Gal4 UAS-smi35A*; α-Dll.
(F) *en-Gal4 UAS-smi35A*; α-Sens.
(F') *en-Gal4 UAS-smi35A*; α-Wg.
(G) *en-Gal4, tubGal80^{ts} UAS-lic*; α-Dll.
(H) *en-Gal4, tubGal80^{ts} UAS-lic*; α-Sens.
(H') *en-Gal4, tubGal80^{ts} UAS-lic*; α-Wg.

examined target gene expression in situations where gene function was reduced by RNAi. Two independent RNAi lines were tested for each gene. In all cases, the RNAi transgene did not detectably alter Wg target gene expression in wing discs. Importantly, all RNAi lines were able to induce other phenotypes, indicating that they are functional. This suggests that *Nek2*, *smi35A*, and *lic* have roles redundant with those of other players in the Wg pathway, providing both an explanation why these genes have not been identified previously and a validation of our strategy to identify redundant factors by overexpression.

Nek2 Interacts with and Phosphorylates Dsh

Ectopic *sens* expression in the wing disc induced by *Nek2* overexpression was largely reduced by coexpression of dominant-negative *lgs* (*lgs^{17E}*), suggesting that *Nek2* modulates *sens* expression through the canonical Wg pathway (Figures 5A and 5B). To explore the mechanism through which Nek2 regulates Wg signaling, we used Nek2 as bait and analyzed by mass spectrometry the proteins with which it coimmunoprecipitated. We found that Dsh, an essential regulator of Wg signaling (Yanagawa et al., 1995; Bilic et al., 2007), copurified with Nek2. Ectopic *sens* expression by *Nek2* was eliminated by *dsh* knockdown (Figure 5C), supporting the notion that *Nek2* functions on or upstream of *dsh* in Wg signaling. To confirm this interaction on the molecular level, we performed coimmunoprecipitation (coIP) experiments and found that the central fragment of Dsh harboring a PDZ domain (Dsh$^{166–382}$) specifically interacted with Nek2 (Figure 5D).

Coexpression of *dsh* with *Nek2* in *Drosophila* Kc cells causes multiple mobility-shifted forms of Dsh on a western blot, which can be eliminated by treating the cell lysate with phosphatase, implying that Nek2 phosphorylates Dsh (Figure 5E). These mobility-shifted species are absent when Nek2 is coexpressed with an N-terminal (1–220), a central (166–382) or a C-terminal (382–623) fragment of Dsh (Figure S4A). However, we could easily detect phosphorylation of Dsh when either Dsh$^{1–340}$ (containing the N terminus and the central domains) or Dsh$^{166–623}$ (containing the central and the C-terminal domains) was coexpressed with wild-type Nek2, but not with the kinase-dead Nek2^{K48M} (Nek2 KD) (Figures 5F and S4B). This suggests that the phosophorylation sites are located in a different domain than the interacting domain. In addition, Nek2 phosphorylates bacterially purified Dsh$^{1–340}$ and Dsh$^{166–623}$ in an in vitro kinase assay, suggesting that these domains are direct targets of Nek2 (Figure 5G).

Since Nek2 might phosphorylate Dsh at both the N and the C termini, we analyzed these two regions separately. Dsh$^{1–340}$ contains a DIX domain and a PDZ domain; both are involved in transducing the canonical Wg signal (Yanagawa et al., 1995; Schwarz-Romond et al., 2007). We thus examined whether Nek2 affected the activity of Dsh$^{1–340}$ in mediating Wg signaling.

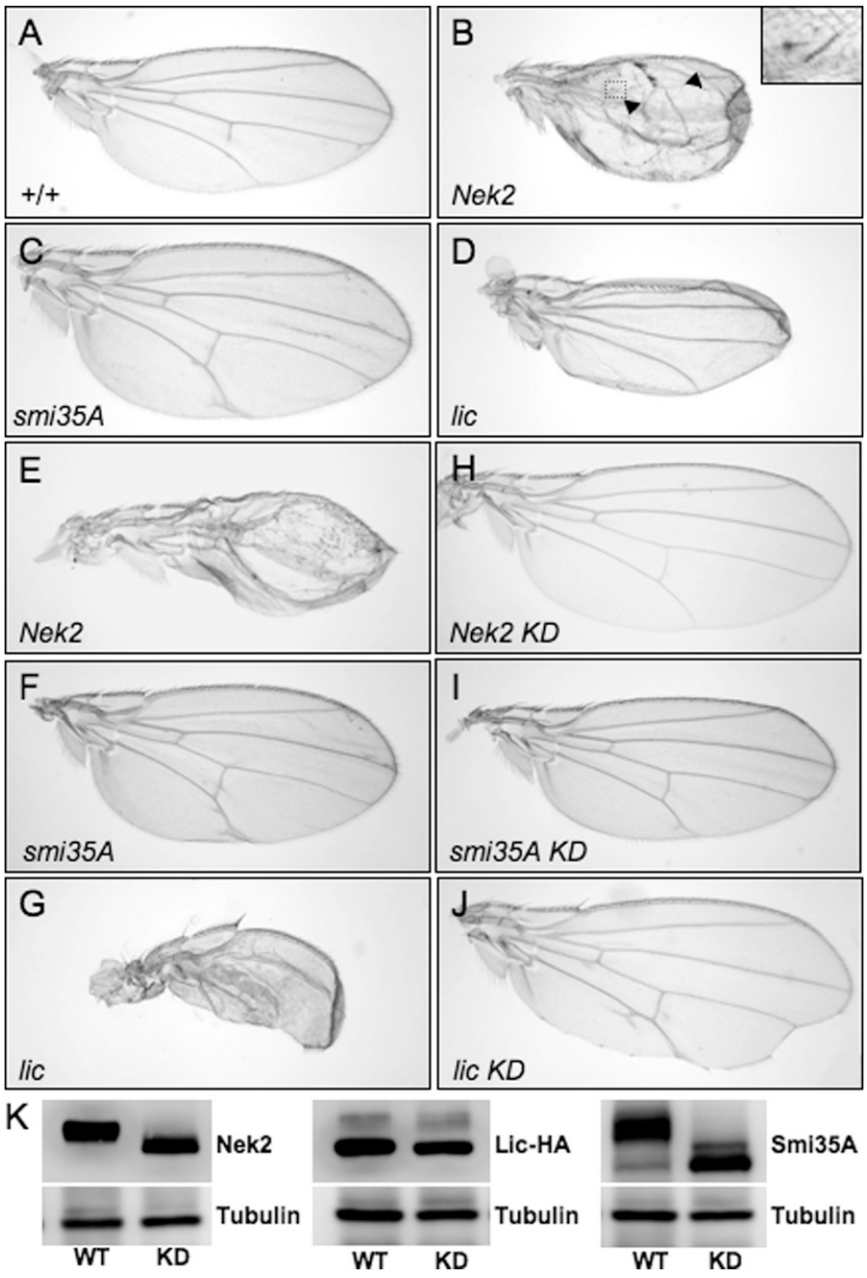

Figure 4. Adult Wing Phenotypes of *Nek2*, *smi35A*, and *lic*

(A–G) Male wings using the *MS1096-Gal4* driver line at 25°C to induce expression. (A) shows *MS1096-Gal4* control. (B) shows *MS1096-Gal4 UAS-Nek2*; severe growth and patterning defects. Arrowheads point toward ectopic sensory bristles. Insert, magnification of the dashed area. (C) shows *MS1096-Gal4 UAS-smi35A*. (D) shows *MS1096-Gal4 UAS-lic*.

(E) shows *salE-Gal4 UAS-Nek2HA*, (F) shows *MS1096-Gal4 UAS-smi35A*, and (G) shows *hh-Gal4 UAS-lic*; flies were raised at 29°C.

(H–J) Expression of kinase-dead (KD) versions using the same drivers and conditions as in (E), (F), and (G), respectively.

(K) Expression of wild-type and mutant forms of *UAS-Nek2*, *UAS-licHA*, and *UAS-smi35A* in Kc cells. Antibodies against Nek2, Smi35A, and HA (for Lic-HA) were used to monitor expression levels.

A luciferase reporter, which contains an endogenous enhancer from the Wg target gene *wingful* (*wf*), responds to Wg signaling in *Drosophila* Kc cells (Song et al., 2010). Compared to full-length Dsh, $Dsh^{1–340}$ does not efficiently activate the *wf* reporter (Figure S5A). Coexpression of $dsh^{1–340}$ with *Nek2*, but not with *Nek2 KD*, synergistically induced the expression of the *wf* reporter, suggesting that Nek2 enhances the activity of $Dsh^{1–340}$ (Figure 6A). We then investigated which domains in $Dsh^{1–340}$ are required for the activation by Nek2 and expressed a series of truncated Dsh constructs (Figure S5B). We found that the regulation of Dsh by Nek2 requires neither a basic motif nor a proline-rich motif flanking the PDZ domain (Penton et al., 2002). However, it does require both the DIX and the PDZ domains. A Dsh construct containing only the DIX and the PDZ domains can be phosphorylated by Nek2 and mediates Wg signaling (Figures 6A and 6B).

Activation of Wg signaling leads to hyperphosphorylation of Dsh at its C terminus and produces a mobility shift on western blots similar to that caused by coexpression of Nek2 with Dsh or $Dsh^{166–623}$ (Figures 5E and 5F) (Yanfeng et al., 2011). By mass spectrometry analysis, we found that $Dsh^{166–623}$ is also phosphorylated at the C terminus when coexpressed with Nek2 in Kc cells. There are six serine residues between amino acids 551 and 557 of Dsh, and four of them can be phosphorylated. Deletion of the C terminus eliminates these phosphorylations, but the DEP domain is dispensable for these modifications (Figure 6C). In addition, a Dsh mutant in which the six serines between residues 551 and 557 are replaced by alanines (Dsh^{6SA}) shows largely reduced mobility shift on western blots when coexpressed with Nek2 (Figure S5C).

Hyperphosphorylation of Dsh promotes its degradation and attenuates Wnt signaling (Wei et al., 2012). To examine whether the identified C-terminal phosphorylation of Dsh affects its stability, we compared the turnover rate of wild-type Dsh and of Dsh^{6SA}. Indeed, Dsh^{6SA} is more stable and activates the *wf* reporter better than wild-type Dsh (Figures 6D and S5D), suggesting that phosphorylation at these residues reduces protein stability but not signaling activity. However, the N-terminal phosphorylations appear to be dominant based on the observed Nek2 function in activating the Wg pathway. In Kc cells, Nek2 has a dynamic effect on wild-type Dsh. While it

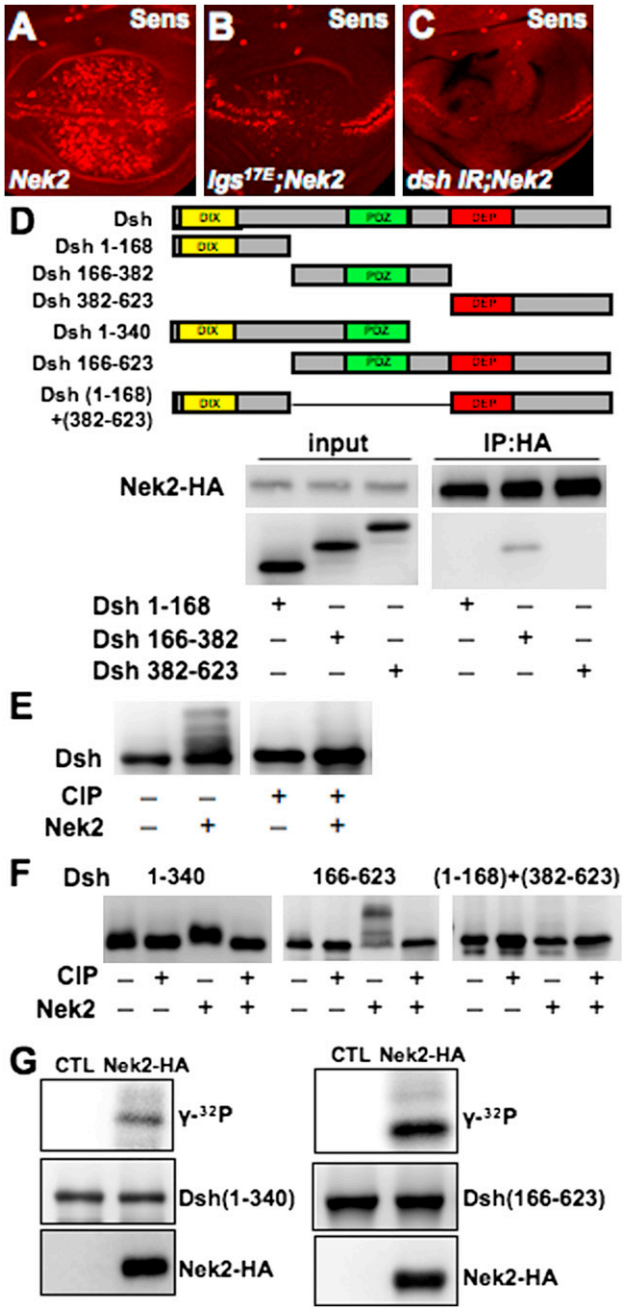

Figure 5. *Nek2* Regulates Wg Signaling via Dsh

(A) Nek2 overexpression by *salE-Gal4* results in ectopic *sens* expression in the wing disc.

(B) Coexpression of dominant negative lgs^{17E} largely reduced ectopic *sens* expression by Nek2.

(C) Dsh RNAi eliminates ectopic *sens* expression by Nek2.

(D) $Dsh^{166–382}$ coimmunoprecitates with Nek2.

(E) Coexpression with Nek2 results in mobility shifts of Dsh in western blot, which is eliminated by CIP treatment.

(F) Nek2 mediates phosphorylation of two truncated Dsh proteins $Dsh^{1–340}$ and $Dsh^{166–623}$.

(G) Nek2 immunopurified from transfected Kc cells can directly phosphorylate $Dsh^{1–340}$ or $Dsh^{166–623}$ (expressed and purified from bacteria) in the in vitro kinase assay.

See also Figure S4.

stimulates the activity of Dsh, Nek2 reduces the protein levels of Dsh when signaling reaches a high level, which may serve as a feedback loop to shape the outputs of Wg signaling (Figure S5E).

Nek2 Is Required to Optimize Wg Signaling Output and Cooperates with CKIε

Although transgenic *Nek2* RNAi does not detectably affect *Drosophila* wing development (Figure S6H), we tested whether *Nek2* is required to promote Wg signal transduction in situations where pathway activity is altered. Ectopic expression of *wg* or *dsh* causes a Wg-specific small eye phenotype. *Nek2* RNAi could partially rescue these phenotypes (Figures S6A–S6F). Similarly, *dsh* misexpression causes ectopic sensory bristles on the wing blade (Figure S6I), and these bristles disappear in the presence of *Nek2* RNAi (Figure S6J), indicating the involvement of endogenous *Nek2* in modulating Wg signaling output.

Mammalian CKIε (encoded by *dco*) phosphorylates Dsh at two different regions, through which it controls both activation and termination of Wnt-induced signaling (Bernatik et al., 2011). Since Nek2 regulates Dsh by a similar mechanism, we examined the possibility of whether *Drosophila* CKIε and Nek2 function redundantly. CKIε, like Nek2, enhances the activity of truncated Dsh in Kc cells. However, we found that the PDZ domain of Dsh was dispensable, while either the basic motif or the proline-rich motif is required for this activation (Figure S6K). Thus, Nek2 and CKIε target different domains or motifs to execute their activating effect on Dsh. When coexpressed in Kc cells, *Nek2* and *CKIε* had an additive effect in activating Wg signaling, both at the basal level and in the presence of Wg ligand (Figures 7A and 7B). Thus, Nek2 and CKIε appear to phosphorylate Dsh at different regions, and, in both cases, the modifications can stimulate Dsh activity. Simultaneous knockdown of *Nek2* and *CKIε* by RNAi in Kc cells showed a stronger reduction of Wg signaling than the knockdown of the individual mRNAs (Figures 7C and 7D). Significantly, all the effects of these constructs on the *wf* reporter were Arm dependent (Figures S6L and S6M). In the *Drosophila* wing, a combination of Nek2 RNAi with a heterozygous *CKIε* mutant (dco^{i3B9}/+) results in loss of sensory bristles along the wing margin, a typical loss-of-Wg-signaling phenotype (Figures 7E–7H). Together, these results suggest that Nek2 can cooperate with CKIε to regulate Dsh and thus Wg signaling.

DISCUSSION

Dominant-Negative Effects and Redundancy

One potential problem of overexpression approaches is the occurrence of dominant-negative effects. Our comparison of the phenotypes induced by RNAi to those of the overexpression lines, suggests a dominant-negative rate of about 40%. A reason for this high number may stem from the fact that many of the genes in our library encode proteins that are part of large multimeric complexes, and overexpression of single components might interfere with the stoichiometry of these complexes. However, the observation that 94 of 371 tested genes caused a strong phenotype when overexpressed, but not when knocked down, highlights the potential of the library for the identification

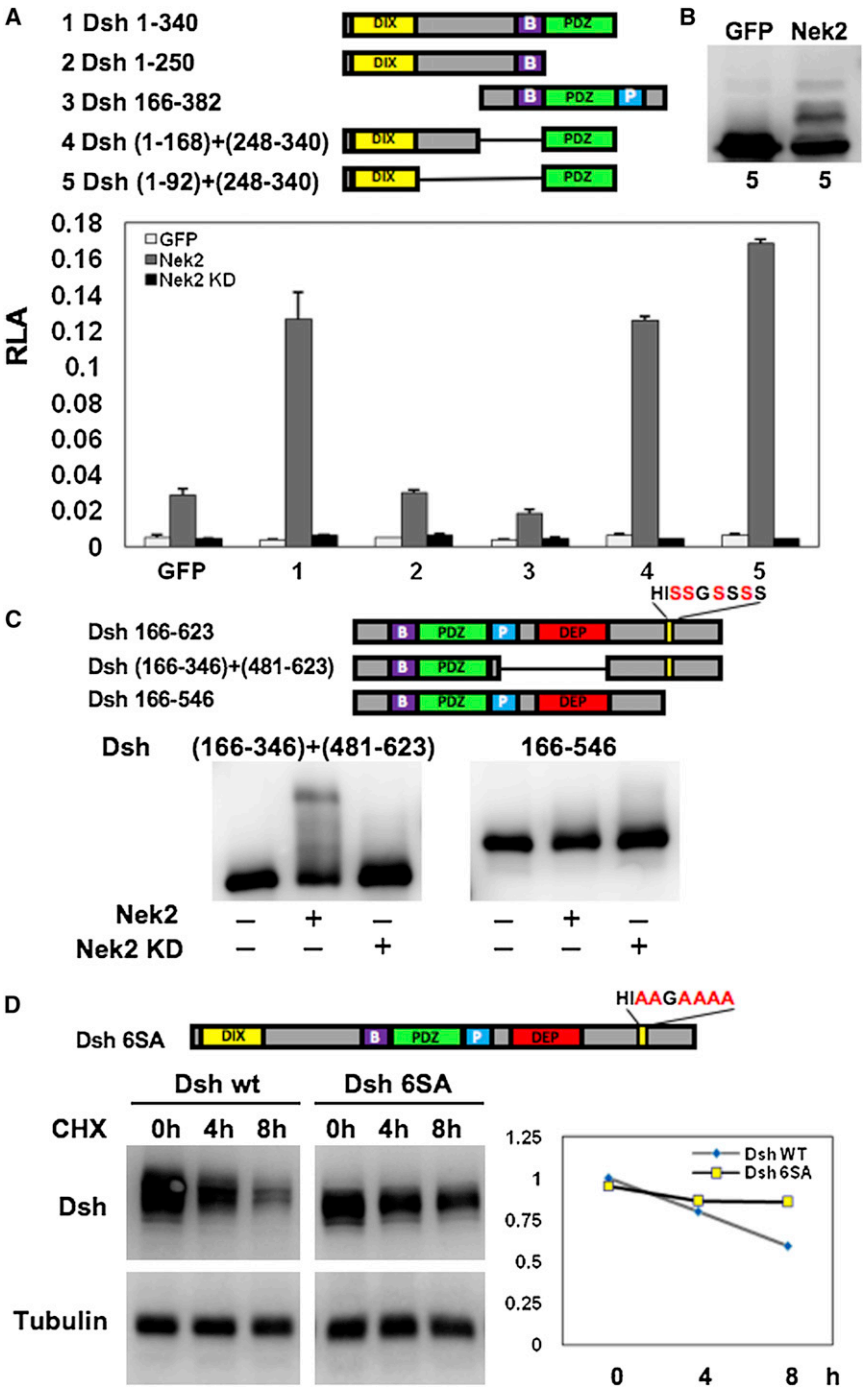

Figure 6. Phosphorylation by Nek2 Has Different Effects on Dsh

(A) The effects of Nek2 on the activities of various truncated Dsh constructs were measured with the *wf* luciferase reporter. Both the DIX domain and the PDZ domain are required for Nek2-mediated stimulation of Dsh activity. Error bars represent SD of samples (n = 3).

(B) Nek2 phosphorylates $Dsh^{(1–92) + (248–340)}$, which is comprised of the DIX domain and the PDZ domain.

(C) Nek2 phosphorylates Dsh at its C terminus. Phosphorylated residues identified in the MS analysis are labeled in red. The DEP domain is not required for these modifications.

(D) The protein stability of transfected wild-type Dsh and Dsh^{6SA} in Kc cells was measured by western blotting after cycloheximide (10 μg/ml) treatment.

See also Figure S5.

of genes that have escaped RNAi or other LOF screens. The association of homologs of some of these genes with human diseases makes them interesting for further testing.

Pathway Crosstalk

When we compared the candidates that were identified by the different phenotypic screens, we noticed considerable overlap. The most significant was found between the screens in the *Myc* and *InR* sensitized backgrounds. This observation is not surprising, since both screens are expected to recover growth-regulating genes. Both pathways affect metabolism and, in particular, translational mechanisms and are thus likely to involve similar sets of genes. However, the sensitized Wg screen also showed significant overlap with these two screens. The Wg screen is functionally different, since it is designed to identify genes that can suppress phenotypes caused by an overactive pathway. Thus, the biological function of the common set of candidates identified in all three screens may be more complex than growth regulation through interference with Myc, insulin, or Wg signaling alone. The high number of interactions among the products of these genes as revealed via STRING analyses underscores the likelihood of a functional relationship between the candidate genes and all three pathways. It needs to be investigated whether this crosstalk occurs at the level of shared pathway components or downstream targets. Interestingly, we find an enrichment of S/T phosphatases within the set of common genes. This indicates that these proteins might be used to fine-tune the different pathways in response to different upstream stimuli. Recent evidence for crosstalk between Wnt signaling and insulin signaling suggests that the signaling protein Insulin Receptor Substrate-1 (IRS-1) is a transcriptional target of *Wnt* signals (Yoon et al., 2010). Also *Myc* genes have been described as direct targets of the Wnt pathway (He et al., 1998; Kuwahara et al., 2010). Furthermore, small molecule inhibitors of PI3K/Akt, an insulin-signaling component, reduced β-catenin-mediated *Myc* expression caused by inhibition of GSK-3β (Baryawno et al., 2010).

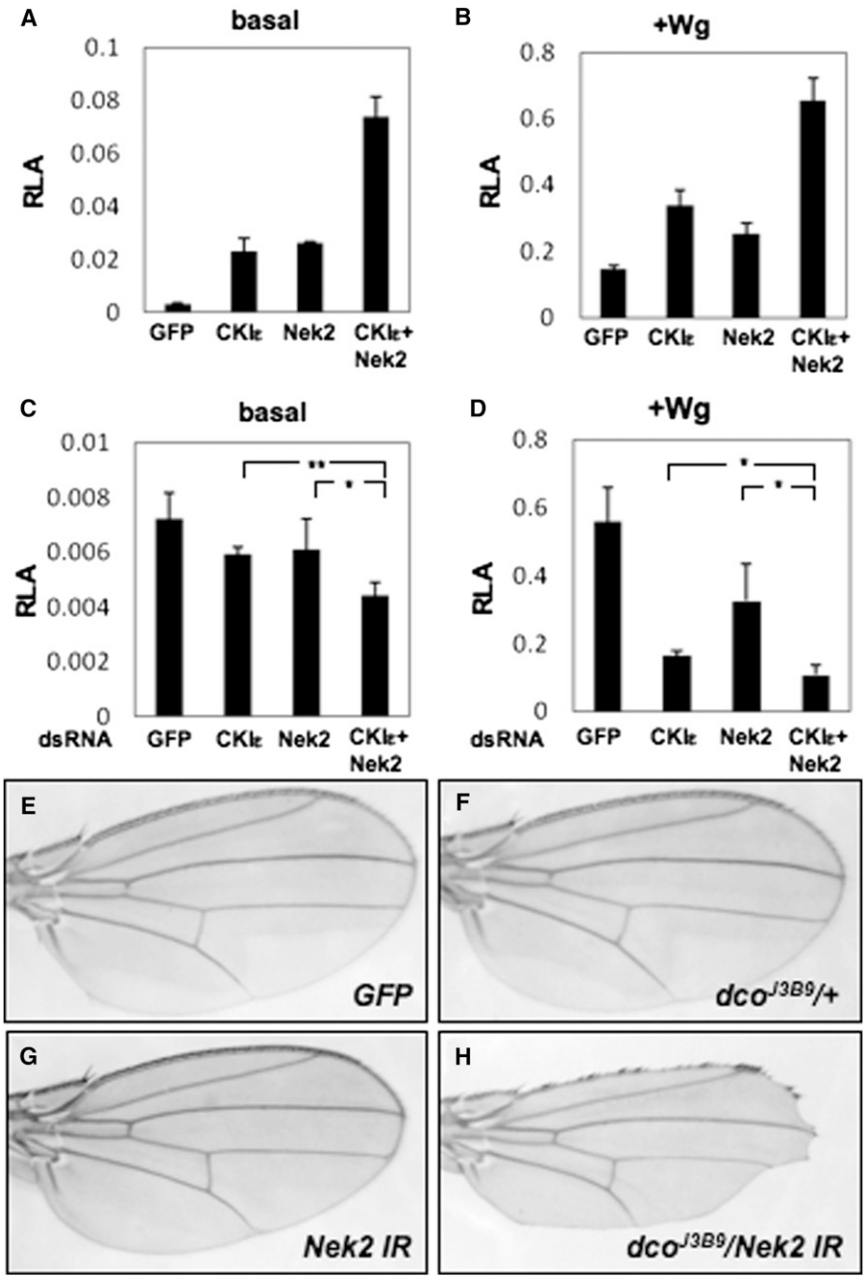

Figure 7. Nek2 and CKIε Have Redundant Roles in Wg Signaling

(A–D) The *wf* luciferase reporter was used as readout for Wg signaling in Kc cells. At both the basal levels (A) and Wg-activated levels (B), overexpression of either *Nek2* or *CKIε* could activate the *wf* luciferase, and coexpression of *Nek2* and *CKIε* could further activate it. In (C), at the basal level, knockdown of either *Nek2* or *CKIε* had very mild effect on Wg signaling, while double knockdown of *Nek2* and *CKIε* led to significant reduction of Wg signaling. As shown in (D), in the presence of Wg, either *Nek2* RNAi or *CKIε* RNAi could suppress Wg signaling levels, while double knockdown of *Nek2* and *CKIε* led to further reduction of Wg signaling. Error bars represent SD of samples (n = 3).

(E–H) Knockdown of *Nek2* by RNAi and *CKIε* with a heterozygous mutant (dco^{j3B9}/+) cause a synergistic effect on the wing morphology and show a typical loss-of-Wg-signaling phenotype. Wings from *sd-Gal4/Y; UAS-GFP*/+ control animals in (E), *sd-Gal4/Y; +;* dco^{j3B9}/+ animals in (F) (100% penetrant, n = 44), *sd-Gal4/Y; +; UAS-Nek2 IR*/+ in (G) (100% penetrant, n = 40), and *sd-Gal4/Y; +;* dco^{j3B9}*/Nek2 IR* animals in (H) (87.5% penetrant, n = 32).

See also Figure S6.

Identification of Wg Pathway Components

In vivo screening of the library resulted in lists of candidate genes that showed an effect in different genetic setups. We expanded the data analysis in a way that allowed specific predictions of gene function. With a focus on the Wg pathway, we aimed to uncover additional signaling components from our in vivo library. By combining hierarchical clustering with predicted STRING protein-interaction data and a genetic screen in a sensitized background, we identified three pathway modifiers.

None of the three kinases caused a phenotype when inactivated by RNAi in vivo, indicating that we would not have identified these genes in an in vivo RNAi screen, lending support to our misexpression strategy. Thus, none of the three genes appears to be strictly required for Wg signaling in vivo, but each one is sufficient to induce Wg-dependent phenotypes. Our results indicate that *Nek2* is a very potent activator, since Wg target genes are strongly upregulated in the wing disc upon *Nek2* overexpression. Misexpression of *smi35A* had a weaker effect and activated the Wg target *Dll* but did not induce *sens*. In contrast, overexpressed *lic* repressed *Dll* and *sens* expression in the wing disc, indicating a negative role for *lic*. Importantly, overexpression of the second MAPK tested, Mekk1, did not affect Wg targets in the wing disc. This indicates that we are not observing a general effect of MAPK signaling, but rather a specific activity of Lic in the Wg pathway in addition to its MAPK function.

Targets for the Identified Kinases in Wg Signaling

All three genes that we identified as potential regulators of the Wg pathway encode S/T kinases, and in each case, a functional kinase domain is required for the observed effects on Wg output. This suggests that the role of Nek2, Smi35A, and Lic is to phosphorylate protein targets within the Wg transduction cascade to enhance or suppress their activity.

Here, we focused on Nek2 and found that it phosphorylates Dsh and plays a dual role in regulating Dsh function. While phosphorylation of the N terminus enhances Dsh-mediated Wg signal

transduction, phosphorylation of the C terminus regulates the half-life of Dsh. The latter function could serve to prevent constitutive activation of the Wg pathway. We further show that Nek2 can cooperate with CKIε to regulate Dsh and Wg signaling. *Nek2* clustered tightly with *arm* and *dsh*, indicating a close functional relationship, which we could confirm for *dsh*. Interestingly, *Nek2* was also found to interact with β-catenin during chromosome separation (Bahmanyar et al., 2008), suggesting that it might also phosphorylate Arm. However, we have not yet observed such an interaction.

CKI and GSK3 phosphorylate NFAT is in human cells (Gwack et al., 2006), and this phosphorylation is primed by the Smi35A homolog DYRK2. Since Smi35A localizes to the cytoplasm, it is unlikely to act in the nuclear branch of the pathway (Lochhead et al., 2003). *smi35A* clusters strongly with *fz* and *fz2*, leading us to speculate that Smi35A might prime one or both receptors for further phosphorylation by other kinases. *lic* clusters strongly with two other S/T kinase genes, *CKIα* and *sgg*, both encoding bona fide negative regulators of Wg signaling. Since *lic* also acts negatively on the pathway, we speculate that Lic might act redundantly with one or both of these kinases.

The kinases themselves could be subject to regulation at the protein level. Indeed, Lic can be phosphorylated in S2 cells by an unknown kinase, while Nek2 and Smi35A are subject to autophosphorylation (Lochhead et al., 2003). In human cells, DYRK1B, a kinase closely related to the human ortholog of Smi35A, is phosphorylated by MKK3, the human ortholog of Lic (Lim et al., 2002). The targets and precise sequence of phosphorylation and dephosphorylation events in the Wg pathway represent challenges for future studies. The conserved nature of the genes and the fact that all three human homologs are implicated in cancer (Miller et al., 2003; Hayward and Fry, 2006; Demuth et al., 2007) suggests that all three kinases, Nek2, Lic/MEK3, and Smi35A/DYRK2, could be important growth regulators that act through regulation of Wg signaling. As such, they may be overactivated in human cancers and cause changes in Wnt signaling, which might contribute to tumor development.

EXPERIMENTAL PROCEDURES

Fly Strains

Flies were raised at 25°C under standard conditions unless stated otherwise. All transgenes were integrated into *y,w,M{eGFP.vas-int.Dm}ZH-2A;+; M{RFP.attP}ZH-86Fb* and are available upon request. Further strains that were used in this study are as follows: *ey-Gal4*, *MS1096-Gal4*, *ey-Gal4;EPdiap1*, *MS1096-Gal4;EPdiap1*, *yw;GMR-Gal4 UAS-InR/CyO*, *yw;ey-Gal4;GMR-upd/TM3*, *yw;GMR-Gal4 UAS-Myc/SM5;2xUAS-Myc/TM6b*, *salE-Gal4 UAS-smo^{7}/CyO*, *en-Gal4/CyO*, *en-Gal4 tubGal80ts*, *salE-Gal4*, *yw hsp-flp;sp/CyO;hh-Gal4/TM6b*, *ey-flp;eyGal4;sev>y+>wg, sev>wg/TM3, UAS-GFP, GMR-Gal4/CyO, sd-Gal4, dco^{i3B9}/TM6b, GMR-Gal4 UAS-dsh/TM6b* (gift from Lei Xue), and *salE-Gal4 UAS-dsh/TM6b*. The kinase-dead versions of *Nek2^{K48M}*, *smi35A^{K227M}*, and *lic^{K75M}* were generated as described in Varjosalo et al., 2008.

Clone Quality

All clones were sequenced, and tagged versions were verified for protein expression. Details will be presented elsewhere (M.B., unpublished data).

Quantification of Screens

According to the phenotypic strength we assigned values from 1 (mild effect) to 4 (lethality) to the observed effects. In screens where we scored enhancement and suppression of the tester phenotype we assigned negative and positive values, respectively, according to phenotypic strength. A complete overview can be found in Table S1, sheet 3. For the screening in apoptosis-deficient backgrounds, we created a category that combines the data of both wing and eye. If the observed size reduction of the adult organ was at least partially blocked by dIAP1 in either background, we assigned a score of 1; if it was not blocked, we assigned a 0.

Wg and E2F Luciferase Reporter Assays

The 10×STAT, dTF12 luciferase, Act5C-Renilla, and PolIII-Renilla luciferase reporters have been previously described. The 6×E2F reporter was constructed by cloning the E2F response element 5′-TCAAATTTCGCGCC TATG-3′ in six tandem repeats in the dTF12 luciferase vector in place of the 12×TCF sites. S2 (for E2f and JakSTAT) and S2R+ (for Wg screen) cells were seeded in white 96-well plates and transfected with 150 ng DNA with 0.45 μl FugeneHD. The DNA mixture contained 2 ng luciferase reporter plasmid, 15 ng Act5C-Renilla plasmid, 50 ng ORF with C-terminal AGT-2×proteinG tag under the control of opIE2 promoter and 83 ng control plasmid. After 2 days, the luciferase activities were measured using the DualGLO luciferase kit (Promega). The luciferase reporter activities were first normalized to the Renilla control values and then normalized to the plate median values. All assays were performed in triplicates.

Bioinformatic Tools

For hierarchical clustering, the screen data were mean-centered and the phenotypes normalized to the same range. The clustering (complete linkage) was performed using uncentered correlation distance metrics with the program Cluster (version 3.0). The Java TreeView (version 1.1.3) software tool was used for data visualization.

Protein interaction predictions were performed with the STRING database, version 8.3 (http://string.embl.de/).

Candidate Gene Scoring System

For the S/T kinase ranking, the hierarchical clustering neighborhood was used to assign a weighted score for each kinase with respect to bona fide pathway components. The two S/T kinases *CKIα* or *gish* are part of a cluster that contains only 33 genes. We assigned a value of 4 to this cluster since it contains two of only four Wg pathway kinases in our library. Genes in clusters I, II, and III were assigned a score of 2 due to strong enrichment of Wg components (cluster II: *pont*, *arm*, *dsh*, *fz*, and *fz2*; five of 17 genes in the cluster, $p < 0.004$, Fisher exact test) or because they contained at least one bona fide S/T-kinase that is implicated in Wg signaling combined with a lower enrichment of Wg components (cluster I: ***CKIIα***, *pan*, *Apc2*, *wg*, *wnt2*, *fz3*, *sgl, Flo*; eight of 78 genes in the cluster, $p < 0.04$) (cluster III: ***sgg***, *fz4*, *rept*, *drl*, *wnt4*, *CtBP*, *wntD*, *mts*; eight of 105 genes in the cluster, $p < 0.06$). STRING database interactions were scored according to the number of predicted interactions (one to three interactions = 1, four to six = 2, more than six = 3). We set a low confidence threshold (0.15) to keep the false-negative rate low. We further assigned a score for observed enhancer effects of the *sev>wg* phenotype of 1. For suppressors, we assigned a higher score (2), since suppression represents a more specific effect.

Immunohistochemistry

The following antibodies were used: mouse anti-Dll (1:500, gift from Ian Duncan), mouse anti-Wg (4D4, 1:500, Hybridoma Bank), guinea pig anti-Sens (1:800, gift from Hugo Bellen), and Alexa Fluor-conjugated secondary antibodies (Molecular Probes).

Transfection, CoIP, Dephosphorylation Assay, and Dual-Luciferase Assay

Cell transfection was performed with Lipofectamine 2000 (Invitrogen) or Effectene (QIAGEN) following the manufacturer's instructions. For coIP, transfected Kc cells were lysed in the lysis buffer (20 mM Na_2HPO_4/NaH_2PO_4, pH 7.4, 150 mM NaCl, 2 mM EDTA, 0.5 mM dithiothreitol [DTT], 0.5 mM Na_3VO_4, 0.5% Triton X-100, 1 protease inhibitor cocktail, and 1 phosphatase inhibitor cocktail; Sigma). Supernatant from cell lysate was incubated with monoclonal anti-HA agarose conjugate (Sigma) at 4°C for 4 hr. After extensive wash with the lysis buffer, the samples were eluted with SDS loading buffer

followed by western blotting. For mass spectrometry analysis, the samples were further washed twice with the lysis buffer, excluding detergent and protease inhibitors, and eluted with 5% formic acid. For the dephosphorylation assay, transfected cells were lysed in a Tris buffer (50 mM Tris-HCl, pH 8.0, 150 mM NaCl, 2 mM EDTA, 0.5 mM DTT, 0.5% Triton X-100, and 1 protease inhibitor cocktail). Supernatant from cell lysate was incubated with or without alkaline phosphatase (CIP) (New England Biolabs) at 37°C for 40 min and analyzed by western blotting. For measurement of the relative luciferase activity, the Dual-Luciferase Reporter Assay kit (Promega) was used.

In Vitro Kinase Assay

$Dsh^{1–340}$ and $Dsh^{166–623}$ were expressed as glutathione S-transferase (GST) fusions from bacterial lysate and were cleaved from GST after purification. Briefly, glutathione beads were incubated with bacterial lysate, washed three times with HENG buffer (20 mM HEPES, pH 7.6, 2 mM EDTA, 0.2% NP40, 10% glycerol, 0.4 mM DTT) containing 1 M NaCl, and washed three times with HENG buffer containing 0.1 M NaCl. Bound proteins were eluted with elution buffer (50 mM Tris-HCl, pH 8.0, 100 mM NaCl, 0.2% NP40, 10% glycerol, 0.4 mM DTT, and 20 mM glutathione), dialysed, and cleaved by protease 3C, and GST was removed by incubation with glutathione beads. Nek2-HA transfected Kc cells were lysed by RIPA buffer. Nek2-HA was immunoprecipitated by anti-HA agarose (Sigma) and washed six times with RIPA buffer and two times with kinase assay buffer (20 mM HEPES, pH 7.6, 50 mM NaCl, 10 mM $MgCl_2$, 10 mM $MnCl_2$, 0.1% NP40, 30 μM cold ATP). For the kinase assay, 15 μl beads were incubated with Dsh substrate and 10 μCi [γ-^{32}P] ATP (Perkin Elmer) in the kinase assay buffer and shaken at 30°C for 2 hr. The proteins were denatured in SDS loading buffer and separated by SDS-PAGE followed by autoradiography or western blotting.

SUPPLEMENTAL INFORMATION

Supplemental Information includes six figures, two tables, and Supplemental Experimental Procedures and can be found with this article online at http://dx.doi.org/10.1016/j.devcel.2013.02.019.

ACKNOWLEDGMENTS

We thank Erika Bach, Peter Gallant, and Ernst Hafen for fly strains, Edy Furger, Nellcia Wang, Eliane Escher, and Sini Miettinen for technical assistance, Stefanie Wanka for help with data analysis, Julia Pepperl and Gerlinde Reim for sharing unpublished data, Andrea Franceschini for help with STRING, and George Hausmann for critical reading of the manuscript. This work was supported by the 973 Program (2011CB943900); the Hundred Talents Program of the Chinese Academy of Sciences; the National Natural Science Foundation of China (31071145); the Deutsche Forschungsgemeinschaft (SCHE 1641/1-1); the University of Zurich's University Research Priority Program, Systems Biology; the National Center of Competence in Research, Frontiers in Genetics; the Swiss National Science Foundation; the Kanton of Zurich; and the Academy of Finland.

Received: October 1, 2012
Revised: January 16, 2013
Accepted: February 28, 2013
Published: April 11, 2013

REFERENCES

Baena-Lopez, L.A., Franch-Marro, X., and Vincent, J.-P. (2009). Wingless promotes proliferative growth in a gradient-independent manner. Sci. Signal. *2*, ra60.

Bahmanyar, S., Kaplan, D.D., Deluca, J.G., Giddings, T.H., Jr., O'Toole, E.T., Winey, M., Salmon, E.D., Casey, P.J., Nelson, W.J., and Barth, A.I.M. (2008). β-Catenin is a Nek2 substrate involved in centrosome separation. Genes Dev. *22*, 91–105.

Baryawno, N., Sveinbjörnsson, B., Eksborg, S., Chen, C.-S., Kogner, P., and Johnsen, J.I. (2010). Small-molecule inhibitors of phosphatidylinositol 3-kinase/Akt signaling inhibit Wnt/beta-catenin pathway cross-talk and suppress medulloblastoma growth. Cancer Res. *70*, 266–276.

Bernatik, O., Ganji, R.S., Dijksterhuis, J.P., Konik, P., Cervenka, I., Polonio, T., Krejci, P., Schulte, G., and Bryja, V. (2011). Sequential activation and inactivation of Dishevelled in the Wnt/beta-catenin pathway by casein kinases. J. Biol. Chem. *286*, 10396–10410.

Bilic, J., Huang, Y.-L., Davidson, G., Zimmermann, T., Cruciat, C.-M., Bienz, M., and Niehrs, C. (2007). Wnt induces LRP6 signalosomes and promotes dishevelled-dependent LRP6 phosphorylation. Science *316*, 1619–1622.

Bischof, J., Maeda, R.K., Hediger, M., Karch, F., and Basler, K. (2007). An optimized transgenesis system for Drosophila using germ-line-specific phiC31 integrases. Proc. Natl. Acad. Sci. USA *104*, 3312–3317.

Bischof, J., Björklund, M., Furger, E., Schertel, C., Taipale, J., and Basler, K. (2013). A versatile platform for creating a comprehensive UASORFeome library in Drosophila. Development. Published online May 14, 2013. http://dx.doi.org/10.1242/dev.088757.

Björklund, M., Taipale, M., Varjosalo, M., Saharinen, J., Lahdenperä, J., and Taipale, J. (2006). Identification of pathways regulating cell size and cell-cycle progression by RNAi. Nature *439*, 1009–1013.

Brand, A.H., and Perrimon, N. (1993). Targeted gene expression as a means of altering cell fates and generating dominant phenotypes. Development *118*, 401–415.

Brunner, E., Peter, O., Schweizer, L., and Basler, K. (1997). pangolin encodes a Lef-1 homologue that acts downstream of Armadillo to transduce the Wingless signal in Drosophila. Nature *385*, 829–833.

Buttitta, L.A., and Edgar, B.A. (2007). Mechanisms controlling cell cycle exit upon terminal differentiation. Curr. Opin. Cell Biol. *19*, 697–704.

Clevers, H. (2006). Wnt/beta-catenin signaling in development and disease. Cell *127*, 469–480.

Cooke, J., Nowak, M.A., Boerlijst, M., and Maynard-Smith, J. (1997). Evolutionary origins and maintenance of redundant gene expression during metazoan development. Trends Genet. *13*, 360–364.

Croce, C.M. (2008). Oncogenes and cancer. N. Engl. J. Med. *358*, 502–511.

Cruz, C., Glavic, A., Casado, M., and de Celis, J.F. (2009). A gain-of-function screen identifying genes required for growth and pattern formation of the Drosophila melanogaster wing. Genetics *183*, 1005–1026.

Demuth, T., Reavie, L.B., Rennert, J.L., Nakada, M., Nakada, S., Hoelzinger, D.B., Beaudry, C.E., Henrichs, A.N., Anderson, E.M., and Berens, M.E. (2007). MAP-ing glioma invasion: mitogen-activated protein kinase kinase 3 and p38 drive glioma invasion and progression and predict patient survival. Mol. Cancer Ther. *6*, 1212–1222.

Dietzl, G., Chen, D., Schnorrer, F., Su, K.-C., Barinova, Y., Fellner, M., Gasser, B., Kinsey, K., Oppel, S., Scheiblauer, S., et al. (2007). A genome-wide transgenic RNAi library for conditional gene inactivation in Drosophila. Nature *448*, 151–156.

Eisen, M.B., Spellman, P.T., Brown, P.O., and Botstein, D. (1998). Cluster analysis and display of genome-wide expression patterns. Proc. Natl. Acad. Sci. USA *95*, 14863–14868.

Gwack, Y., Sharma, S., Nardone, J., Tanasa, B., Iuga, A., Srikanth, S., Okamura, H., Bolton, D., Feske, S., Hogan, P.G., and Rao, A. (2006). A genome-wide Drosophila RNAi screen identifies DYRK-family kinases as regulators of NFAT. Nature *441*, 646–650.

Hayward, D.G., and Fry, A.M. (2006). Nek2 kinase in chromosome instability and cancer. Cancer Lett. *237*, 155–166.

He, T.C., Sparks, A.B., Rago, C., Hermeking, H., Zawel, L., da Costa, L.T., Morin, P.J., Vogelstein, B., and Kinzler, K.W. (1998). Identification of c-MYC as a target of the APC pathway. Science *281*, 1509–1512.

Jensen, L.J., Kuhn, M., Stark, M., Chaffron, S., Creevey, C., Muller, J., Doerks, T., Julien, P., Roth, A., Simonovic, M., et al. (2009). STRING 8—a global view on proteins and their functional interactions in 630 organisms. Nucleic Acids Res. *37*(Database issue), D412–D416.

Jia, J., Amanai, K., Wang, G., Tang, J., Wang, B., and Jiang, J. (2002). Shaggy/GSK3 antagonizes Hedgehog signalling by regulating Cubitus interruptus. Nature *416*, 548–552.

Jia, J., Tong, C., Wang, B., Luo, L., and Jiang, J. (2004). Hedgehog signalling activity of Smoothened requires phosphorylation by protein kinase A and casein kinase I. Nature *432*, 1045–1050.

Kuwahara, A., Hirabayashi, Y., Knoepfler, P.S., Taketo, M.M., Sakai, J., Kodama, T., and Gotoh, Y. (2010). Wnt signaling and its downstream target N-myc regulate basal progenitors in the developing neocortex. Development *137*, 1035–1044.

Lim, S., Jin, K., and Friedman, E. (2002). Mirk protein kinase is activated by MKK3 and functions as a transcriptional activator of HNF1alpha. J. Biol. Chem. *277*, 25040–25046.

Lochhead, P.A., Sibbet, G., Kinstrie, R., Cleghon, T., Rylatt, M., Morrison, D.K., and Cleghon, V. (2003). dDYRK2: a novel dual-specificity tyrosine-phosphorylation-regulated kinase in Drosophila. Biochem. J. *374*, 381–391.

Miklos, G.L., and Rubin, G.M. (1996). The role of the genome project in determining gene function: insights from model organisms. Cell *86*, 521–529.

Miller, C.T., Aggarwal, S., Lin, T.K., Dagenais, S.L., Contreras, J.I., Orringer, M.B., Glover, T.W., Beer, D.G., and Lin, L. (2003). Amplification and overexpression of the dual-specificity tyrosine-(Y)-phosphorylation regulated kinase 2 (DYRK2) gene in esophageal and lung adenocarcinomas. Cancer Res. *63*, 4136–4143.

Penton, A., Wodarz, A., and Nusse, R. (2002). A mutational analysis of dishevelled in Drosophila defines novel domains in the dishevelled protein as well as novel suppressing alleles of axin. Genetics *161*, 747–762.

Rørth, P., Szabo, K., Bailey, A., Laverty, T., Rehm, J., Rubin, G.M., Weigmann, K., Milán, M., Benes, V., Ansorge, W., and Cohen, S.M. (1998). Systematic gain-of-function genetics in Drosophila. Development *125*, 1049–1057.

Schwarz-Romond, T., Fiedler, M., Shibata, N., Butler, P.J.G., Kikuchi, A., Higuchi, Y., and Bienz, M. (2007). The DIX domain of Dishevelled confers Wnt signaling by dynamic polymerization. Nat. Struct. Mol. Biol. *14*, 484–492.

Song, H., Goetze, S., Bischof, J., Spichiger-Haeusermann, C., Kuster, M., Brunner, E., and Basler, K. (2010). Coop functions as a corepressor of Pangolin and antagonizes Wingless signaling. Genes Dev. *24*, 881–886.

St Johnston, D. (2002). The art and design of genetic screens: Drosophila melanogaster. Nat. Rev. Genet. *3*, 176–188.

Varjosalo, M., Björklund, M., Cheng, F., Syvänen, H., Kivioja, T., Kilpinen, S., Sun, Z., Kallioniemi, O., Stunnenberg, H.G., He, W.-W., et al. (2008). Application of active and kinase-deficient kinome collection for identification of kinases regulating hedgehog signaling. Cell *133*, 537–548.

Verheyen, E.M., and Gottardi, C.J. (2010). Regulation of Wnt/beta-catenin signaling by protein kinases. Dev. Dyn. *239*, 34–44.

Wei, W., Li, M., Wang, J., Nie, F., and Li, L. (2012). The E3 ubiquitin ligase ITCH negatively regulates canonical Wnt signaling by targeting dishevelled protein. Mol. Cell. Biol. *32*, 3903–3912.

Yanagawa, S., van Leeuwen, F., Wodarz, A., Klingensmith, J., and Nusse, R. (1995). The dishevelled protein is modified by wingless signaling in Drosophila. Genes Dev. *9*, 1087–1097.

Yanfeng, W.A., Berhane, H., Mola, M., Singh, J., Jenny, A., and Mlodzik, M. (2011). Functional dissection of phosphorylation of Disheveled in Drosophila. Dev. Biol. *360*, 132–142.

Yoon, J.C., Ng, A., Kim, B.H., Bianco, A., Xavier, R.J., and Elledge, S.J. (2010). Wnt signaling regulates mitochondrial physiology and insulin sensitivity. Genes Dev. *24*, 1507–1518.